Magazine of Civil Engineering. 2019. 92(8). Pp. 142–154
Инженерно-строительный журнал. 2019. № 8(92). С. 142–154

Magazine of Civil Engineering

ISSN 2071-0305

journal homepage: http://engstroy.spbstu.ru/

DOI: 10.18720/MCE.92.12

Effects of model-based design and loading on responses of base-isolated structures

A. Dushimimana[a]*, A.A. Niyonsenga[b], G.J. Decadjevi[a], L.K. Kathumbi[c]
[a] Ondokuz Mayis University, Samsun, Turkey
[b] Shaoxing University, Shaoxing, China
[c] Pan African University, Institute for Basic Science, Technology and Innovation, Nairobi, Kenya
** E–mail: chenkodu432@gmail.com*

Keywords: numerical methods, dynamic loads, time of implementation, loading nature, seismically isolated structures, model-based design

Abstract. Numerical studies for a structural dynamic system are performed in Matlab and Simulink environments. Six different earthquakes filtered and corrected using Seismosignal software, are used as seismic loads during implementation. In the first part of this study, the fourth order Runge-Kutta based Matlab code (RK4M) and Simulink Model-Based Design (SMD) are appropriately developed. Both RK4M and SMD are used to solve the governing equations for single storey structure isolated by Lead Core Rubber Bearing (LCRB). The second part compares the developed modelling methods in terms of outputs' accuracy and Time of Implementation (TI). It is shown that both methods agree well in terms of resulting floor accelerations and displacements with slight but justifiable average differences of only 1.3 and 0.98 % respectively; thus, indicating that any of these techniques can be adopted. However, concerning TI, it is observed that SMD is in general quicker to display results as compared to the developed RK4M, which is approximately 58s longer. This leads to suggesting that SMD can be more effective, particularly for earthquakes with long-duration, and most importantly for cases where time is a governing factor during implementation. Besides, long-period and long-duration earthquakes are observed to have particular influence on structural behaviour. This reveals a need for special consideration requirements that are currently not taken into account.

1. Introduction

Simulink provides a block diagram environment that is used as a platform for model-based design. Matlab provides an environment for developing codes relevant to the type of model that is being investigated. The time required to develop the code can be high due to a number of factors, which mainly depend on the type of the structure being modelled. Contrary to Matlab environment, Simulink-model based design can save time of implementation, mainly because of the presence of built-in-blocks that are easy and ready to use. Both Matlab and Simulink environments can be used to solve governing equations of motion of a structural dynamic system, such as active and passive seismically isolated structures.

A significant number of solution methods for differential equations governing a dynamic motion of passive seismically isolated structures have been adopted in the existing literature. For example, a number of researchers have adopted the Wilson Theta method [1, 2], Newmark Beta method [3–6], and Runge-Kutta Methods [3, 4, 7–11]. The latter has been observed to be the most stable, modern and popular method according to most of researchers [3, 4]. However, there is a substantial need to conduct comparative studies on the performance level of methods adopted during implementation. Two of the major performance factors that can be considered are: the accuracy of the results and time required to display desired responses.

Despite a significant number of existing programming software such as Matlab, Python, and Ansys; there is still a substantial need to clarify the easy and fastest software and technique. Such a software and technique can reduce the time required to obtain structural responses during implementation, while providing

Dushimimana, A., Niyonsenga, A.A., Decadjevi, G.J., Kathumbi, L.K. Effects of model-based design and loading on responses of base-isolated structures. Magazine of Civil Engineering. 2019. 92(8). Pp. 142–154. DOI: 10.18720/MCE.92.12

Душимимана А., Ньонсенга А.А., Декаджеви, Г.Дж., Катумби Л.К. Влияние модельно-ориентированного проектирования и нагрузки на отклики конструкции с изолированным фундаментом // Инженерно-строительный журнал. 2019. № 8(92). С. 142–154. DOI: 10.18720/MCE.92.12

accurate results in a short time. Matlab has been significantly reported to possess the ability to perform better compared to other existing programming software used in solving the governing differential equations for dynamic motion of seismic base isolation systems [3, 4, 11]. With this in mind, the use of Matlab and its embedded part (Simulink) to predict the system accuracy and TI can be more reasonable than using other existing programming software. Particularly, when examining a seismic isolation system, significant studies have previously reported Matlab to be effective [7, 12]. Furthermore, studies by use of Simulink have been conducted by a significant number of researchers for solving the governing equations of dynamic motion of seismically isolated structures [12–17]. Specifically, Numerical studies have been conducted on LCRB performance by using both Matlab and Simulink including [7, 8, 12, 18] among others.

The potentiality of adopting Simulink to solve the governing differential equations in seismically isolated structures was reported in [12], where calibration of isolator parameters under long-period motions was mainly targeted. In [19], governing equations of a dynamic system were solved by four different types of methods including Matlab and Simulink environments. It was reported that the latter can be a better technique as it only requires knowledge of blocks' functionality already designed for solving related equations without much knowledge in coding or/and advanced mathematics.

Despite a large number of the existing literature about numerical studies on seismically isolated structures with LCRB, there has been a remarkable gap in searching for the best technique to use during the numerical analysis. Such a technique can be easier, faster and be seen as a prerequisite for practical use, most importantly for projects which prioritize the accuracy of the responses while saving TI. In [20], a numerical algorithm that is based on the finite element model of contact and step-by-step analysis method was used to model a base-structure contact interaction during dynamic loads. It was observed that such a modelling technique can save time compared to the existing well-known iteration algorithm. Similar studies for the sake of developing a modelling method with time-saving, cost-effective, and energy efficient properties were also conducted in [21, 22]. However, these studies were not addressing seismically isolated structures. Therefore, there is a need to develop a modelling technique with the above properties for seismically isolated structures.

With regard to the loading nature, a substantial number of studies have been conducted adopting the normal or short-period earthquakes, as well as short-duration [5, 23–25]. However, a few studies have considered the effect of long-period earthquakes on responses of isolated structures [26–29]. Most notably, the combining effect of long-period and long-duration earthquakes on isolated structures seems to have not been investigated in the existing literature.

In this study, authors aim to compare SMD and RK4M techniques in terms of accuracy of results and TI of resulting responses for a structure that is seismically isolated by LCRB. The accuracy of these techniques is checked based on the resulting outputs, while TI is controlled by carefully recording the elapsed time for each method. Besides, the study aims to examine the effect of earthquake nature on the responses of seismically isolated structures, particularly the long-period and long-duration earthquakes. The main contribution of this work lies in assessing the easiest to use and time-saving technique, which authors believe can mainly be beneficial in reducing the time required during numerical analysis of seismically isolated structures. Besides, the study contributes in revealing the severity of long-period and long-duration earthquakes on seismically isolated structures.

The remainder of this study is structured as follows. Section 2 presents the methodology and description of numerical simulations, and governing differential equations solved in both RK4M and SMD techniques; in Section 3, numerical case study is provided for deep understanding of section 2 and its applicability; in section 4, numerical case study results are discussed; and conclusions are drawn in Section 5.

2. Methods

2.1. Defining Governing Equations

The governing equations for dynamic motion of structures with multiple degrees of freedom, fixed or controlled by LCRB at the base level can be detailed as follow [12, 30]:

The equation of a fixed base structure exposed to seismic load can be expressed as

$$[M_S]\{\ddot{U}_S\}+[C_S]\{\dot{U}_S\}+[K_S]\{U_S\}=-[M_S]\{R\}(\ddot{u}_g). \quad (2.1)$$

A structure isolated by LCRB at its base level can be governed by equations (2.2) and (2.3).

a) The superstructure part is governed by the equation:

$$[M_S]\{\ddot{U}_S\}+[C_S]\{\dot{U}_S\}+[K_S]\{U_S\}=-[M_S]\{R\}(\ddot{u}_g+\ddot{u}_b), \quad (2.2)$$

where $[M_S]$, $[C_S]$ and $[K_S]$ are the mass, damping and stiffness matrices of the superstructure, respectively; $\{U_S\} = \{U_1, U_2, \ldots, U_j\}^T$, $\{\dot{U}_S\}$ and $\{\ddot{U}_S\}$ are the unknown floor displacement, velocity and acceleration

vectors respectively; U_j is the lateral displacement of j^{th} floor relative to the base mass; $\ddot{u}_b$ and $\ddot{u}_g$ are the relative acceleration of base mass and earthquake ground acceleration respectively; and $\{R\}$ is the vector of influence coefficients.

b) For the base floor level of the building, the equation of motion can be expressed as:

$$m_b\ddot{u}_b + F_b - k_1u_1 - c_1\dot{u}_1 = -m_b\ddot{u}_g, \tag{2.3}$$

where m_b and F_b are base mass and restoring force developed in the isolation system, respectively; k_1, c_1, u_1, and $\dot{u}_1$ are the stiffness, damping, displacement, and velocity of first storey floor. The value for hysteretic restoring force F_b can be calculated as shown below:

$$F_b = c_b\dot{u}_b + \alpha k_b u_b + (1-\alpha) f_y Z. \tag{2.4}$$

In equation (2.4), f_y refers to yield force, α stands for the ratio of post-yield to pre-yield stiffness; k_b, c_b, u_b, $\dot{u}_b$, are stiffness, damping, displacement, and velocity of the bearing, respectively; and Z is a component of Wen's non-linear model shown in (2.5).

$$\dot{Z} = \left[A\dot{u}_b - \beta|\dot{u}_b|Z|Z|^{n-1} - \tau\dot{u}_b|Z|^n \right] u_y^{-1}, \tag{2.5}$$

where u_y is yield displacement, and can be calculated for particular structure as described in ASCE 41-13. β, A and τ are dimensionless parameters which are defined based on laboratory experiments. n is a constant value, and this controls the transition from elastic to plastic behavior of the model.

The above equations can be solved by one of the most commonly used techniques such as Runge-Kutta 4th order algorithm, Wilson Theta Method, and Newmark Beta Method, assuming a linear variation over smaller time interval (dt = 0.001s). Properties of LCRB such as stiffness (k_b), damping (c_b), damping ratio (ξ_b), yield strength (F_y), normalized yield strength (Fo), and yield displacement (u_y) can be calculated based on following equations [12, 31]:

$$k_b = \left(\frac{2\cdot\pi}{T_b} \right)^2 \cdot \left(M_{sup} + m_b \right), \quad w_b = \frac{2\cdot\pi}{T_b}; \tag{2.6}$$

$$c_b = 2\cdot\xi_b \cdot \left(M_{sup} + m_b \right) \cdot w_b, \quad g = 9.81; \tag{2.7}$$

$$F_y = Fo\cdot W, \quad u_y = \frac{F_y}{k_b}, \quad \xi_b = 0.15, \quad Fo = 0.0159, \quad W = M\cdot g, \tag{2.8}$$

where m_b, w_b, T_b, g and W are bearing mass, natural frequency, natural period, acceleration of gravity and total weight of structure, respectively. M_{sup} is the total mass of superstructure.

2.2. RK4M Technique

In this research, RK4M is adopted to solve the equations (2.1) to (2.3), as shown by a number of researchers [3, 4, 10, 18]. This algorithm is based on Runge-Kutta 4th order, which is applied in Matlab environment by coding line by line. The equations defining this algorithm are shown in (2.9) to (2.13),

$$y_{k+1} = y_k + \frac{h(f_1 + 2f_2 + 2f_3 + f_4)}{6}, \tag{2.9}$$

where f_1, f_2, f_3, f_4, are slopes of the given function within a single time step size (h). y_k and y_{k+1} are the previous and current variables for each step size h.

$$f_1 = f(t_k, y_k); \tag{2.10}$$

$$f_2 = f\left(t_k + \frac{h}{2}, y_k + \frac{h}{2} f_1 \right); \tag{2.11}$$

$$f_3 = f\left(t_k + \frac{h}{2}, y_k + \frac{h}{2} f_2 \right); \tag{2.12}$$

$$f_4 = f\left(t_k + h,\ y_k + hf_3\right). \tag{2.13}$$

The above algorithm will output first order ODEs to be solved by one of the Matlab built-in-function such as ode45, ode23s among others. In this method, preallocation is used wherever possible in order to speed up the code execution time. This process is made through preallocating maximum amount of space required for an array. However, RK4M can only provide displacements and velocities. Therefore, accelerations can be derived from the already obtained velocity values by using one of the existing popular techniques known as numerical derivative. This can be implemented either through forward difference, backward difference, or central difference methods shown in equations (2.14), (2.15), and (2.16) respectively [3, 11].

$$f'\left(x_k\right) \approx \frac{f\left(x_{k+1}\right) - f\left(x_k\right)}{x_{k+1} - x_k}; \tag{2.14}$$

$$f'\left(x_k\right) \approx \frac{f\left(x_k\right) - f\left(x_{k-1}\right)}{x_k - x_{k-1}}; \tag{2.15}$$

$$f'(x_k) \approx \frac{f(x_{(k+1)}) - f(x_{(k-1)})}{(x_{(k+1)} - x_{(k-1)})}. \tag{2.16}$$

In this study, forward difference method is adopted and the Matlab built-in function (*diff*) is used to solve equation (2.14). Additionally, input parameters for RK4M (mass of structure $[M_s]$, structure stiffness $[K_s]$) can be generalized as shown in equations (2.17) and (2.18).

$$\left[M_S\right] = \begin{bmatrix} m_1 & 0 & 0 & 0 & 0 & 0 \\ 0 & m_2 & 0 & 0 & 0 & 0 \\ 0 & 0 & m_3 & 0 & 0 & 0 \\ 0 & 0 & 0 & \ldots & 0 & 0 \\ 0 & 0 & 0 & 0 & \ldots & 0 \\ 0 & 0 & 0 & 0 & 0 & m_i \end{bmatrix} \left(\mathrm{Kg}\right); \tag{2.17}$$

$$\left[K_S\right] = \begin{bmatrix} k_1 + k_2 & -k_2 & 0 & 0 & 0 & 0 \\ -k_2 & k_2 + k_3 & -k_3 & 0 & 0 & 0 \\ 0 & -k_3 & k_3 + k_4 & -k_3 & 0 & 0 \\ 0 & 0 & \ldots & \ldots + \ldots & \ldots & 0 \\ 0 & 0 & 0 & \ldots. & \ldots + \ldots & -k_i \\ 0 & 0 & 0 & 0 & -k_i & k_i \end{bmatrix} \left(\mathrm{N/m}\right), \tag{2.18}$$

where i is the number of floors in the investigated structure. In this study, damping matrix $[C_s]$ was derived from $[M_s]$ and $[K_s]$ based on Rayleigh Method [7, 12], which is defined as shown in (2.19).

$$\left[C_S\right] = \alpha_o\left[M_S\right] + \alpha_1\left[K_S\right]. \tag{2.19}$$

The coefficients α_0 and α_1 can be obtained by solving equation (2.20)

$$\frac{1}{2}\begin{bmatrix} \frac{1}{w_i} & w_i \\ \frac{1}{w_j} & w_j \end{bmatrix} \begin{Bmatrix} \alpha_0 \\ \alpha_1 \end{Bmatrix} = \begin{Bmatrix} \xi_i \\ \xi_j \end{Bmatrix}, \tag{2.20}$$

where w_i, w_j, ξ_i, ξ_j, are natural frequencies and damping ratios of fixed base structure for i^{th} and j^{th} mode respectively. Damping ratios at i^{th} and j^{th} are assumed to be similar to facilitate the calculation of the concerned coefficients [2, 12].

2.3. SMD Technique

Contrary to the above mentioned RK4M method, SMD is adopted to solve equations (2.1) to (2.3) by logically connecting Simulink built-in blocks. Referring to researchers in [12, 32–37], equations (2.1) to (2.3) can be combined into a single equation (2.21) to represent the structure as a whole, and then transformed into a state-space form of first order equations i.e., a continuous-time state-space model of the system as shown in equations (2.22) and (2.23).

$$[m]\{\ddot{u}(t)\}+[c]\{\dot{u}(t)\}+[k]\{u(t)\}=[d]\{f_{\oplus}(t)\}; \tag{2.21}$$

$$\dot{z}(t)=[A_c]z(t)+[B_c]\{f_{\oplus}(t)\}; \tag{2.22}$$

$$\{y(t)\}=[C]z(t)+[D]\{f_{\oplus}(t)\}. \tag{2.23}$$

The components shown in the above equations are explained in Table 2.1

Table 2.1 Definition of state space model components.

Variant parameter symbol	Definition	Matrix size
z	Space vector	$n_1\ by\ 1$
$\dot{z}$	States	$n_1\ by\ n_1$
$f_{\oplus}$	Input force vector	$r_1\ by\ 1$
y	Desired responses vector	$m_1\ by\ 1$
A_c	Feedback matrix	$n_1\ by\ n_1$
B_c	İnput matrix	$n_1\ by\ r_1$
$[C]$	Output influence matrix	$m_1\ by\ n_1$
$[D]$	Direct transmission matrix	$m_1\ by\ r_1$
$[d]$	İnput influence matrix	$n_2\ by\ r_1$

$n_1 = 2n_2$; n_2 is the number of independent coordinates. r_1 is the number of inputs, m_1 is the number of outputs. $[d]$ characterizes the locations and type of known inputs $f_{\oplus}(t)$ [8, 12, 18, 38, 39].

$$[A_c]=\begin{bmatrix}[0] & [I]\\ -[m]^{-1}[k] & -[m]^{-1}[c]\end{bmatrix}; \tag{2.24}$$

$$[B_c]=\begin{bmatrix}[0]\\ m^{-1}[d]\end{bmatrix}; \tag{2.25}$$

$$\{z(t)\}=\begin{bmatrix}u(t)\\ \dot{u}(t)\end{bmatrix}. \tag{2.26}$$

The sizes of matrices $[C]$ and $[D]$ can be adjusted depending on the desired output [16]. The Simulink-Model Based Design can be constructed as shown below:

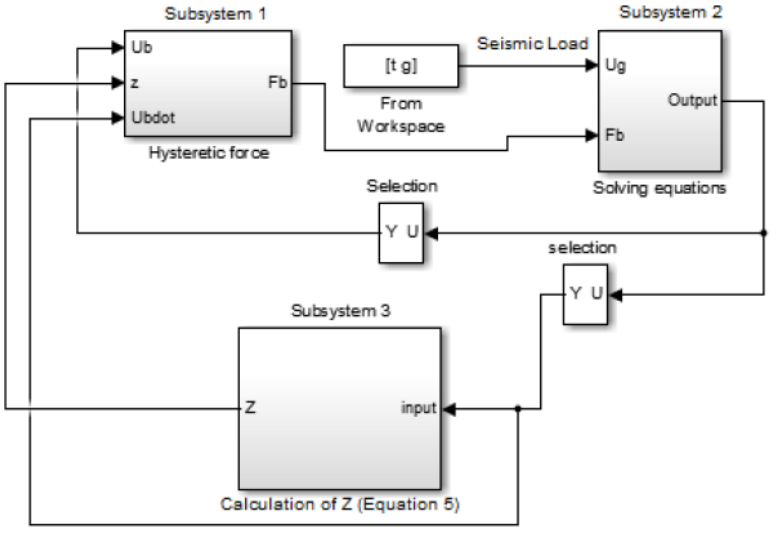

Figure 2.1. Simulink Master Block diagram for modeling isolated structure by LCRB isolator.

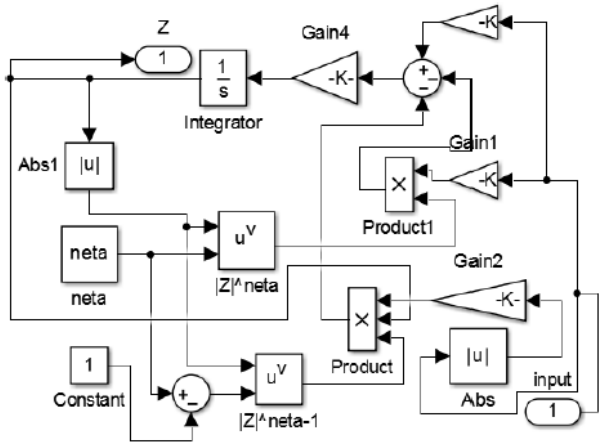

Figure 2.2. Calculation of Z (Subsystem 3).

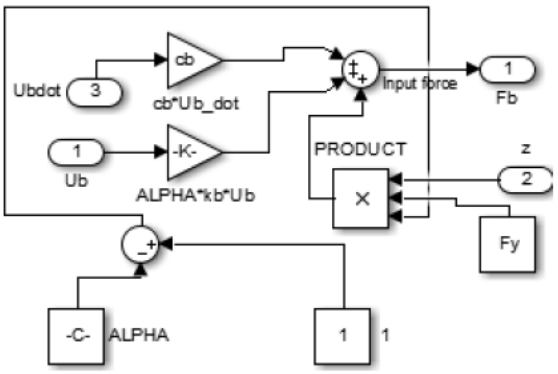

Figure 2.3. Calculation of Fb (Subsystem 1).

Blocks used to form SMD are chosen based on references [3, 12] Model configuration parameters are set based on the recommendations shown in [15] for solving equation of a dynamic system.

2.4. Numerical case study

In this study, the responses of an isolated one storey structure under various earthquakes are investigated. The engineering data for the above structure are as follows: m_1 = 29 485 kg; m_b = 6800 kg, k_1 = 11 912 KN/m. The basic dynamic properties of the investigated structure are natural period: T_{n1} = 0.1s; frequency: F_{n1} = 10 Hz, and damping ratios: ξ_{n1} = 0.05. The above characteristics have been previously adopted in [16]. Furthermore, the geometry properties of the considered lead core rubber bearing are: i) diameter = 700 mm, ii) thickness of plates: 56 mm, iii) total thickness of elastomer = 120 mm (each with 4 mm), iv) single steel shim thickness = 3.1 mm. These data have been also adopted in [40].This structure is exposed to a total of six earthquakes downloaded from PEER strong ground motions [41], filtered and corrected using Seismosignal Software (SS). The characteristics of these earthquakes are summarized in Table 2.2. The results for TI strongly depend on the type of computer being used during implementation. Therefore, the properties of the computers used in this study are as follow: Computer brand: hp ProBook 4540s, Processor: Intel(R) Core(TM) i3-3110M CPU@ 2.40GHz, system type: 64-bit Operating System, and RAM; 4.00GB.

Table 2.2. Characteristics of used earthquakes.

Earthquake Name	PGA (m/s^2)	PGV(m/s)	Duration (s)
Elcentro	3.42	0.32	56.52
Düzce	1.29	0.11	42.29
Chuestsu	2.23	0.23	59.96
Capemembe	1.47	0.42	286.65
Iwate	1.78	0.10	179.97
Kobe	8.18	0.82	49.93

3. Results and Discussions

3.1. Differences Between RK4M and SMD for the Resulting Responses of Structure

Looking at peak values in Table 3.1 and Figure 3.1 to 3.9, it appears that both methods resulted in nearly similar responses with small but justifiable differences. For example, in Table 3.1, based on the results from RK4M under Elcentro earthquake, the maximum responses of BFA, TFA, BFD and TFD were observed to be 3.04 m/s^2, 3.09 m/s^2, 0.08 m, 0.08 m, whereas those from SMD were 3.07 m/s^2, 3.10 m/s^2,0.09 m, 0.101 m, respectively. It follows that the average acceleration and displacement differences from both methods were approximately 1 and 1.5 %, respectively. These slight differences may have been caused by from workspace block in SMD, which failed to reproduce the input earthquake acceleration. It can therefore be suggested that this block needs revision for better performance.

Similar interpretations can be done on the results from other earthquakes. For example, a careful analysis on responses from both methods under Duzce, Chuestsu, Capemembe, Iwate and Kobe earthquakes indicates that the average acceleration and displacement differences were: 1 and 1 %, 1.5 and 0 %, 1.5 and 1.4 %, 2 and 1 %, and 1.5 and 1 %, respectively. Similar to Elcentro earthquake, these differences can be attributed to the inefficiency of from workspace block to reproduce the input earthquake acceleration. Overall, the average acceleration differences from both methods under all the earthquakes can be estimated to be 1.3 %, whereas for the displacements the average difference can be estimated to be 0.98 %.

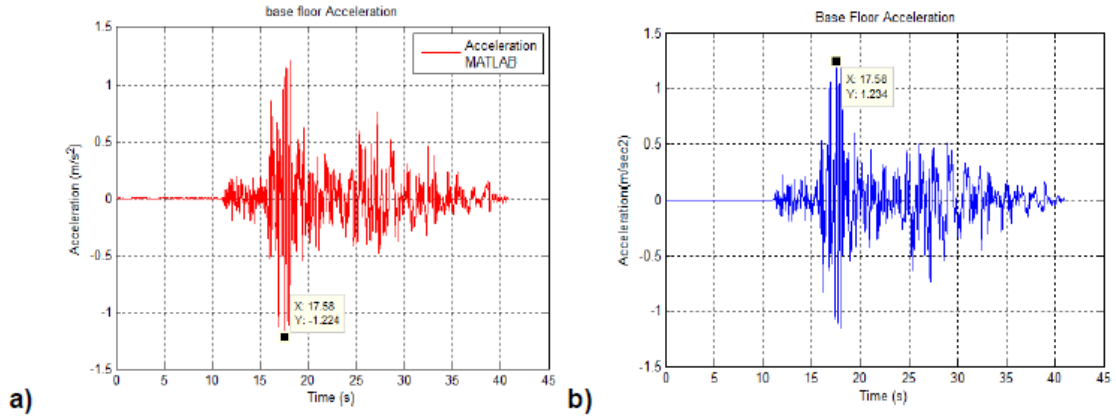

Figure 3.1. Base floor accelerations under Duzce Earthquake: a) RK4M, and b) SMD.

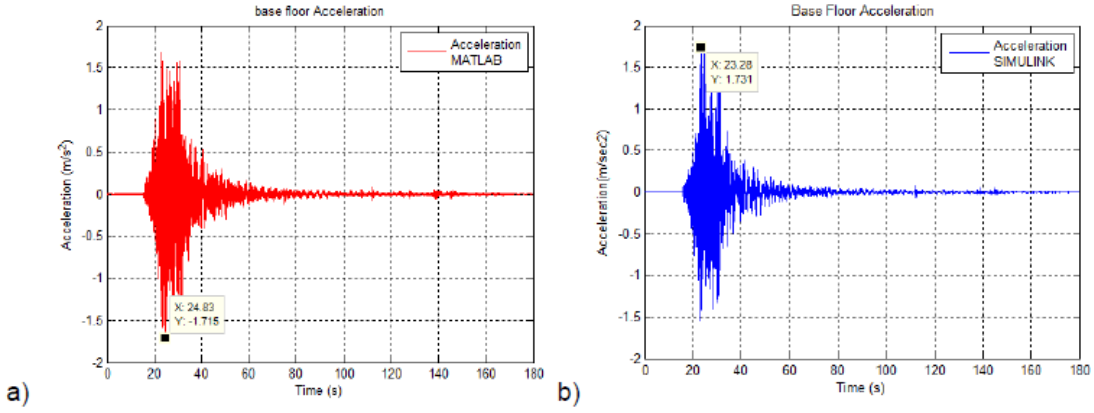

Figure 3.2. Base floor accelerations under Iwate Earthquake: a) RK4M, and b) SMD.

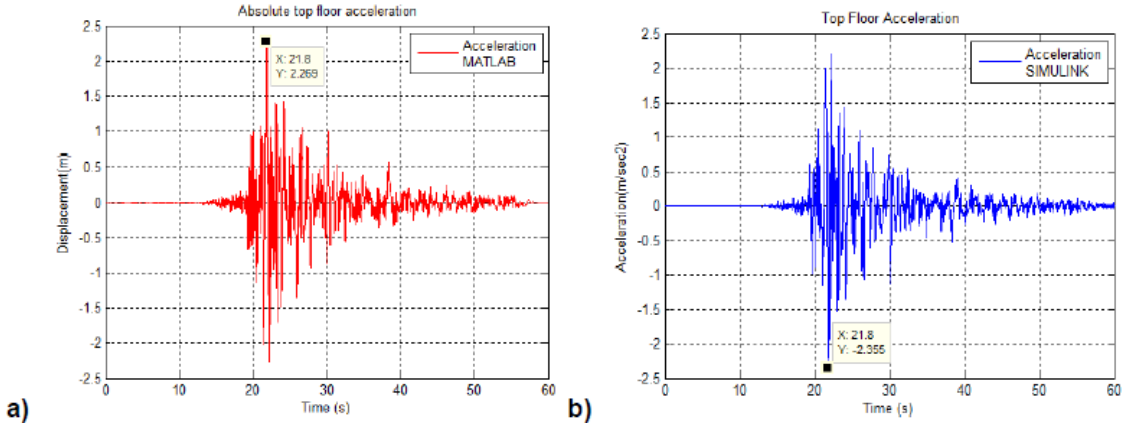

Figure 3.3. Top floor accelerations under Chuestsu Earthquake: a) RK4M, and b) SMD.

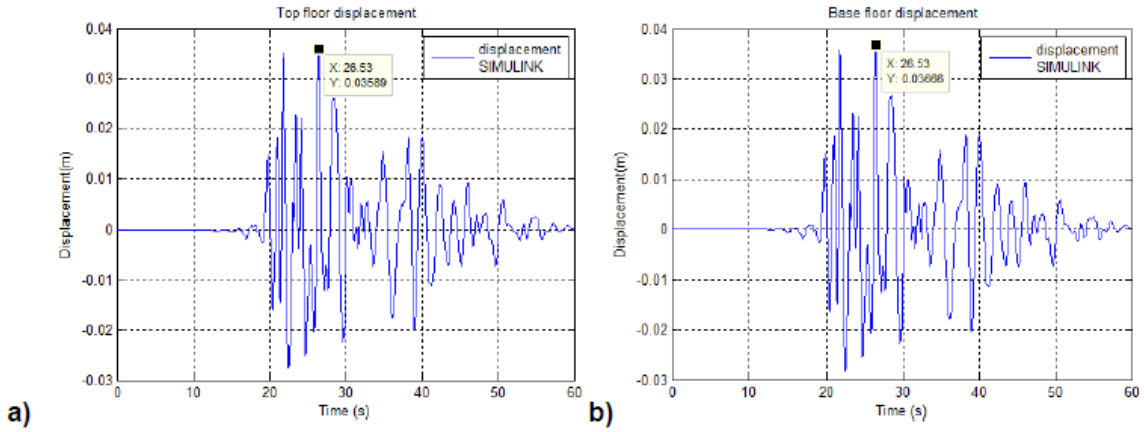

Figure 3.4. a) Top and b) Base floor displacements under Churstsu earthquake for SMD.

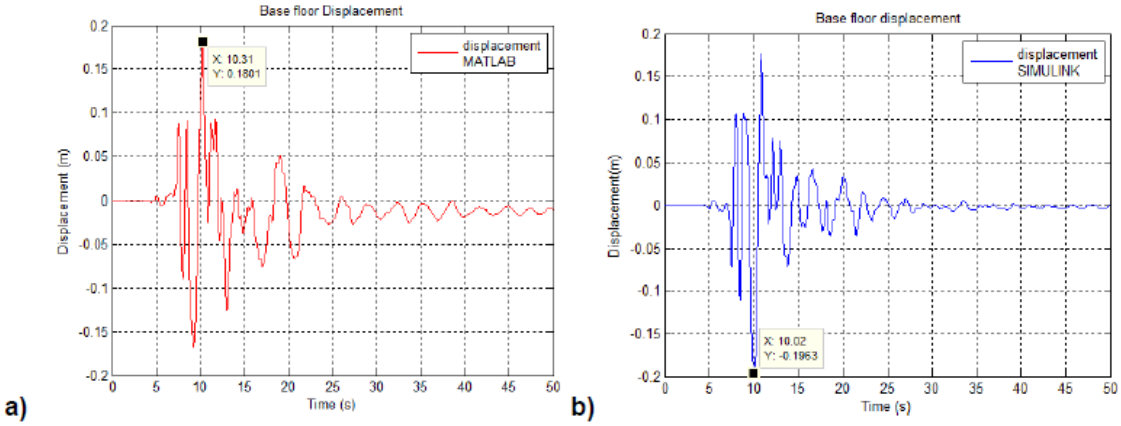

Figure 3.6. Base floor displacements under Kobe Earthquake: a) RK4M, and b) SMD

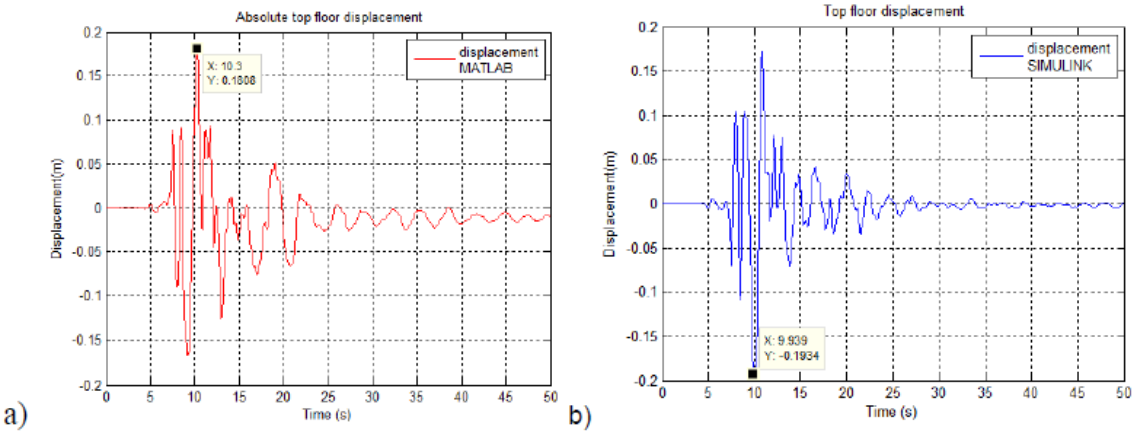

Figure 3.6. Top floor displacements under Kobe Earthquake: a) RK4M, and b) SMD.

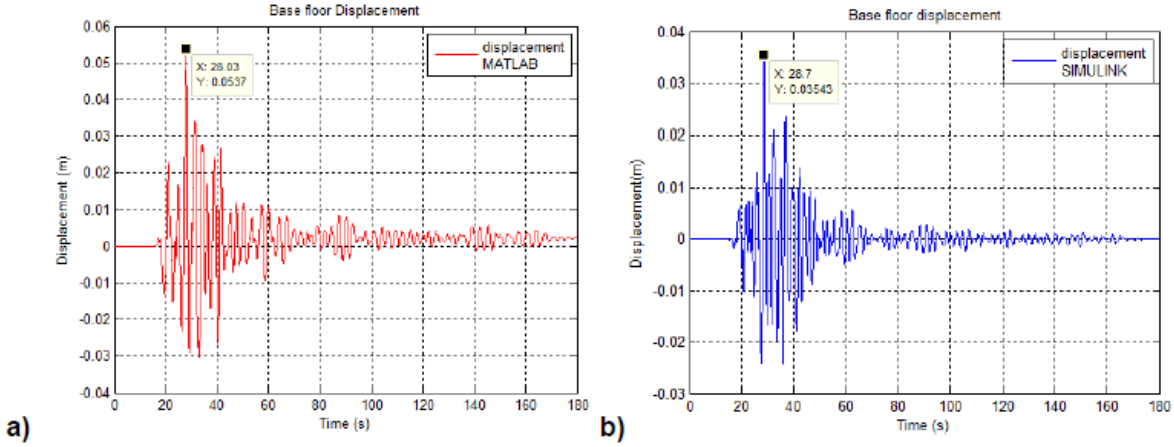

Figure 3.7. Base floor displacements under Iwate Earthquake: a) RK4M, and b) SMD.

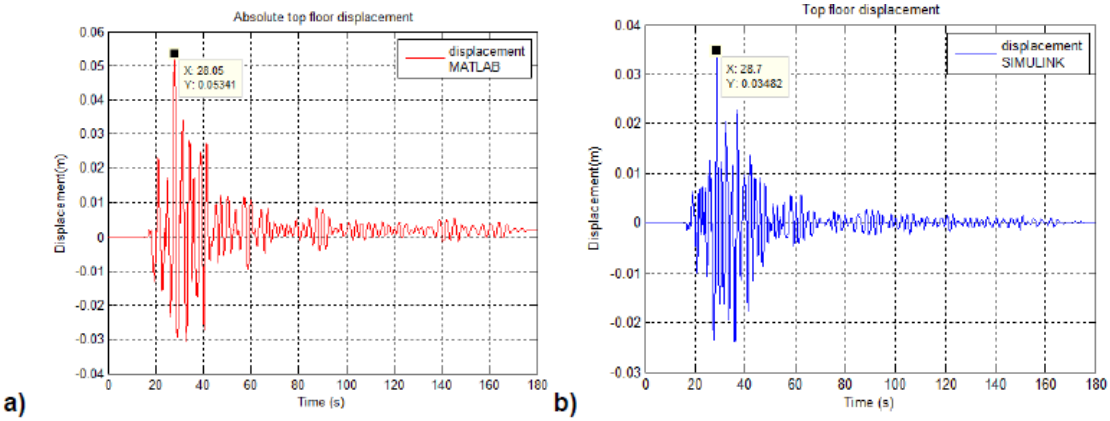

Firure 3.8. Top floor displacements under Iwate Earthquake: a) RK4M, and b) SMD

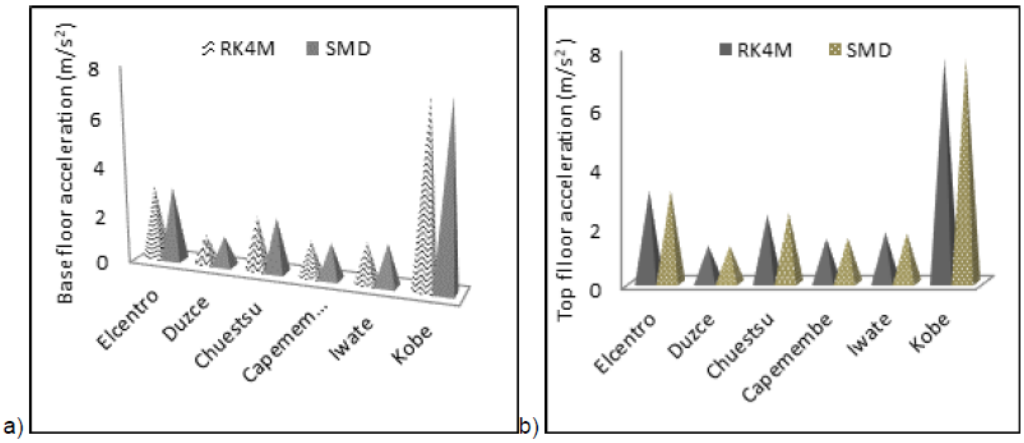

Figure 3.9. Comparison of maximum base and top floor accelerations from RK4M and SMD methods.

Concerning the time instants (*ti*) for the occurrence of maximum peak responses, it can be observed from Figure 4.1 to 4.8 that RK4M and SMD methods kept *ti* approximately similar for each response. For example, under Duzce earthquake, both methods succeeded in providing maximum base floor acceleration values at exactly similar *ti* of 17.58s as shown in Figure 4.1. It follows from this observation that there was a *ti* difference of approximately 0s. Under Chuestsu, Kobe and Iwate earthquakes, the *ti* for maximum top and base displacements under both methods were nearly 29s, 10s, and 28s, respectively. This uniformity in *ti* for top and base floor responses indicates a good agreement between the used methods and high performance of the bearing. This similarity in *ti* reveals that both top and base floor displacements of the structure moved with reduced storey drifts. This observation can clearly be seen in Figure 4.4 where maximum displacements were similarly equal, and occurred at exactly *ti* of 28.53s for both floors.

Table 3.1. Comparison of RK4M and SMD results for one storey structure.

Earthquake Name/PGA/Direction		Period (Tb)	SR and TI	MATLAB (RK4M)	SIMULINK (SMD)	RK4M&SMD Difference
Elcentro	Direction: NS	3	BFA (m/s^2)	3.04	3.07	0.01
			TFA (m/s^2)	3.09	3.10	0.01
			BFD (m)	0.08	0.09	0.01
PGA (m/s^2)	3.42		TFD (m)	0.08	0.10	0.02
			TI (s)	17.54	1.51	16.03
Duzce	Direction: NS	3	BFA (m/s^2)	1.22	1.23	0.01
			TFA (m/s^2)	1.25	1.24	0.01
			BFD (m)	0.03	0.02	0.01
PGA (m/s^2)	1.29		TFD (m)	0.03	0.02	0.01
			TI (s)	14.44	1.56	12.88
Chuestsu	Direction: NS	3	BFA (m/s^2)	2.25	2.27	0.02
			TFA (m/s^2)	2.28	2.27	0.01
			BFD (m)	0.04	0.04	0.00
PGA (m/s^2)	2.41		TFD (m)	0.04	0.04	0.00
			TI (s)	25.91	1.63	24.28
CAPEMEMBE	Direction: NS	3	BFA (m/s^2)	1.47	1.49	0.02
			TFA (m/s^2)	1.49	1.50	0.01
			BFD (m)	0.31	0.30	0.01
PGA (m/s^2)	1.47		TFD (m)	0.31	0.29	0.02
			TI (s)	82.29	2.11	80.18
IWATE	Direction: NS	3	BFA (m/s^2)	1.71	1.73	0.02
			TFA (m/s^2)	1.69	1.67	0.02
			BFD (m)	0.05	0.04	0.01
PGA (m/s^2)	1.78		TFD (m)	0.05	0.04	0.01
			TI (s)	203.98	1.94	202.04
KOBE	Direction: NS	3	BFA (m/s^2)	7.47	7.45	0.02
			TFA (m/s^2)	7.53	7.52	0.01
			BFD (m)	0.18	0.19	0.01
PGA (m/s^2)	8.18		TFD (m)	0.18	0.19	0.01
			TI (s)	12.75	1.55	11.20

NS: North-South, PGA: Peak ground Acceleration, Tb: Isolation period, SR: Structural responses, TI: Time of Implementation, BFA: Absolute base floor acceleration, TFA: Absolute Top floor acceleration, BFD: Base floor displacement, TFD: Absolute Top floor displacement.

3.2. Differences in TI for RK4M and SMD Methods

On the other hand, the differences in TI were observed to be significantly pronounced between RK4M and SMD methods. TI required for RK4M to display responses were observed to be 17.54, 14.44, 25.91, 82.29, 203.98, and 12.75s under Elcentro, Duzce, Chuestsu, Capemembe, Iwate and Kobe earthquakes, respectively. However, a much more pronounced difference was observed for TI when SMD is adopted. That is, TI for SMD to display responses were observed to be 1.51, 1.56, 1.63, 2.11, 1.94, and 1.55s under Elcentro, Duzce, Chuestsu, Capemembe, Iwate and Kobe earthquakes, respectively. The observations from RK4M and SMD indicate that both methods resulted in differences of 16.03, 12.88, 24.28, 80.18, 202.04, and 11.20s under Elcentro, Duzce, Chuestsu, Capemembe, Iwate and Kobe earthquakes, respectively. In other words, the average TI value required for displaying responses under all earthquakes was approximately 59.50s for RK4M, while that of SMD was approximately 1.72s. It follows from this observation that there was nearly 58s (or 97 %) difference of TI between the used methods when all earthquakes are counted. Particularly, long-duration earthquakes like Capemembe and Iwate were observed to consume much more time for RK4M than for SMD as can be observed in Figure 3.10.

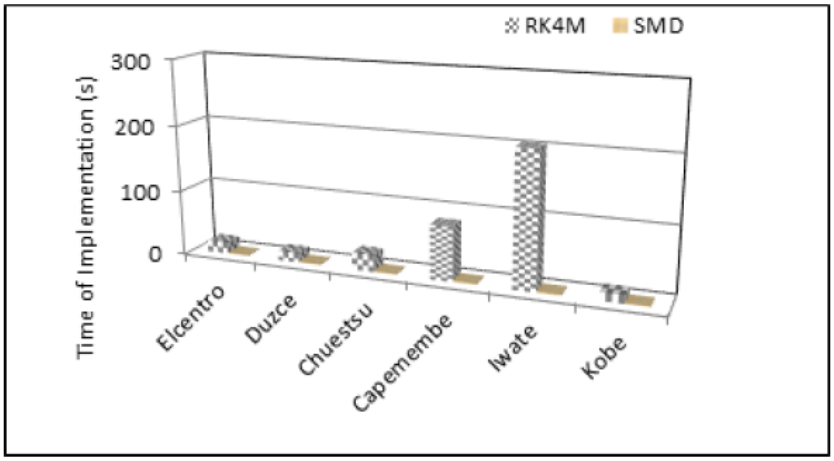

Figure 3.10. Comparison of TI for RK4M and SMD under various earthquakes.

This pronounced difference provided insights about the paramount importance of adopting SMD rather than RK4M for such earthquakes. Overall, the substantial percentage difference in TI under both methods paves the way for suggesting SMD to be more effective than RK4M. The adoption of SMD is reasonable in a way that time is a governing factor in real life. For example, if a project is to take time *t* for its accomplishment when RK4M adopted, the adoption of SMD can substantially reduce that *t*. This reduction will result not only from the above mentioned percentage difference in TI, but also from saving time required to develop RK4M code, and sift through lines of the code in order to understand. This will probably result in labor cost-savings through substantial reduction of required working hours.

3.3. Effect of Earthquake Nature on the Resulting Responses

The results in Table 3.1 provide information about the effect of earthquake nature on the responses of the investigated structure. Interestingly, under Capemembe earthquake with PGA of 1.47 m/s^2, base and top floor displacements were observed to be higher than those resulting from Kobe earthquake with PGA of 8.18 m/s^2. For example, base and top floor displacements from RK4M under Capemembe earthquake appeared to be similar and equal to 0.31 m, whereas those under Kobe earthquake were similar and equal to 0.18 m. The fact that Capemembe is a long-period and long-duration earthquake in its nature could have been the underlying cause of higher displacements compared to Kobe earthquakes'. Analysis from Seismosignal Software "intensity parameters" indicates that Capemembe earthquake displacement (shown in Figure 3.11) has a predominant period of 3.4s, which makes this earthquake to be of long-period nature. Furthermore, Figure 3.11 shows that this earthquake lasted for nearly 300s, which makes it of long-duration earthquake nature. It is evident from time duration of this earthquake that it possesses many load cycles. Because it had been previously reported that the number of load cycles contributes to bearing damage [42], the presence of many load cycles for this earthquake can dramatically cause severe damage. It can be observed from Table 3.1 and Figure 3.12 that due to the combining effect of long-period and long-duration characteristics of the Capemembe, the maximum displacements of the structure were amplified nearly 10 times the earthquake maximum displacement.

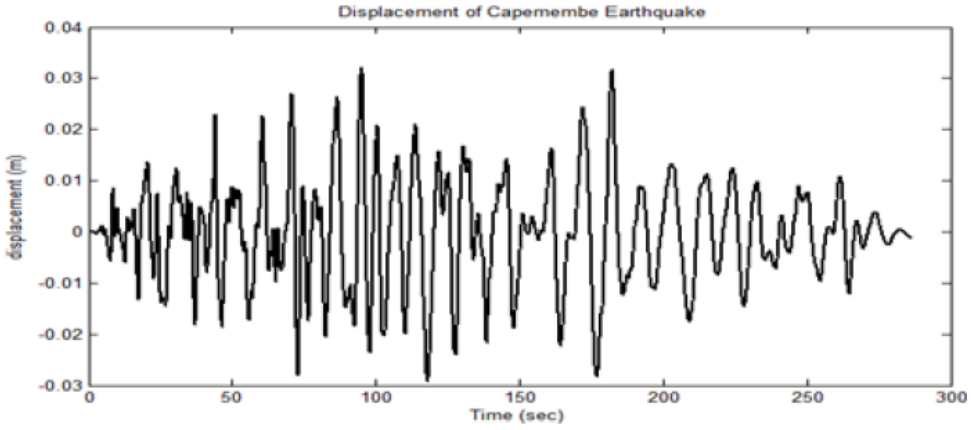

Figure 3.11. Displacement of Capemembe Earthquake.

Another observation from Figure 3.11 is the repetition of peak displacements with almost equal magnitudes (i.e. nearly 0.03 m for each peak) at approximately 72.9, 95.1, 118, 177, and 182.4s. In fact, these peaks occurred in-between 50 and 100 s, 100 and 150s, and 150 and 200s. This shows that earthquake severity on the structure lasted for long, which probably led to development of large isolator strains, and hence large floor displacements. With regard to EN 1337-3 [43], the formula for calculating shear strains (ε_{qE}) due to earthquake-imposed horizontal displacement is $\varepsilon_{qE} = d_{bd} / T_q$, where d_{bd} is the earthquake imposed design displacement and T_q is the total thickness of the elastomer.

Previous studies [40, 44, 45], have reported that large displacements due to strong ground motions can cause the bearing to experience larger shear strains in the elastomer than the allowed strains (100 %) as per EN 1337-3 [43]. This is in agreement with the shear strains obtained from strong Kobe earthquake (i.e.150 %). However, it seems that long-period long-duration earthquakes can also cause excessive shear strains in the bearing regardless of their PGA as shown by Capemembe earthquake which causes shear strains in the elastomer of about 258 %. With regard to previous study conducted by [40], shear strains exceeding 125 % can cause the tensile stresses above $5G$, where G is the shear modulus of the elstomer. However, the code provisions limit tensile stresses in the bearing up to $2G$ in BS EN 15129 [46] and EN 1337-3 [43], up to $2–3G$ in ASHTO [47], and up to $1G$ in JRA [48]. It is, therefore, evident that shear strains from Capemembe earthquake can cause tensile stresses higher than those recommended in the codes. This can lead to development of cracks, buckling, and even rupture during seismic loadings, thus leading to poor performance of isolation system. Therefore, it is of paramount importance to mention that the isolator material properties should be adjusted to avoid such unusual displacements from the aforementioned combining effect of long-period and long-duration earthquakes. This can reduce the cost of damage due to large displacements as had been previously reported by [21], and can result in a sustainable bearing able to last for long period of time.

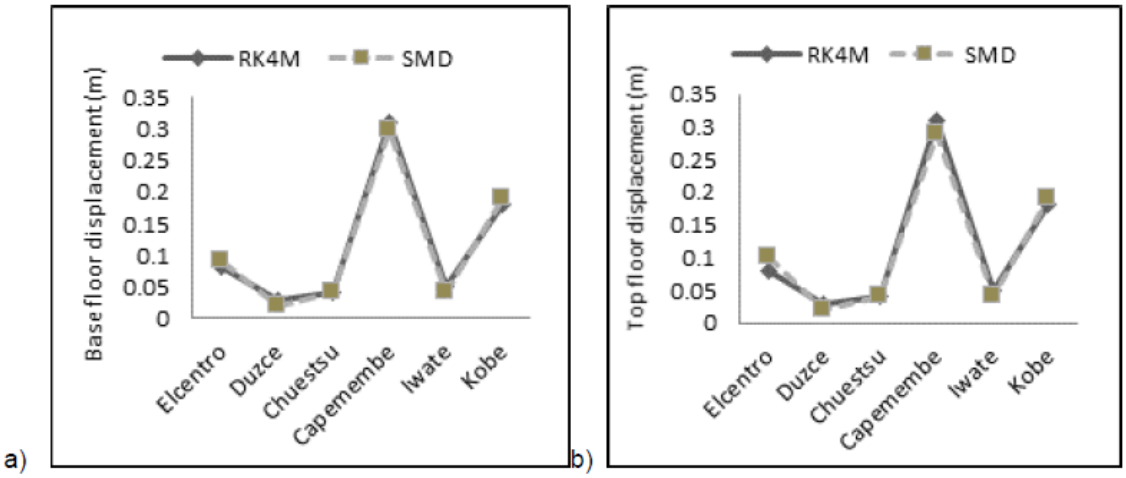

Figure 3.12. Comparison of base and top floor displacements under various earthquakes.

Overall, there was occurrence of nearly similar values of both top and base floor responses under both methods as shown in Figure 3.1 to 3.9. This similarity indicates not only a good agreement between RK4M and SMD methods, but also the effective performance of the bearing. This is because the similarity in top and base responses normally indicates that the structure moves as a rigid body, thus preventing interstorey drifts as well as unwanted cracks during earthquake. However, SMD was observed to be more time-saving than RK4M. On the other hand, the unusual floor displacements observed for long-period and long-duration earthquakes can be an indication that special consideration requirements are necessary. For example, changing the bearing material constituents can be one of possible solutions.

4. Conclusion

In this study, RK4M and SMD methods were adopted for solving differential equations governing a dynamic motion of a structure isolated by LCRB. The resulting responses from both methods were analyzed and compared. For comparison purposes, one storey structure exposed to earthquakes (filtered and corrected using SS) with significant differences in their PGA was investigated. Besides, the combining effect of long-period and long-duration earthquakes on the isolated structures was analyzed. The major findings are listed as shown below:

1. The dynamic responses of the investigated structure were nearly similar under both RK4M and SMD methods. This indicates that there was a good agreement between these methods. However, the developed SMD modelling technique was found to be much easier and faster than RK4M. Therefore, SMD is shown to be a promising method for saving time required during numerical analysis of seismically isolated structures, and can be adopted especially for projects where time is a governing factor.

2. For all earthquakes, the average acceleration difference from both methods was estimated to be 1.3 %, whereas the average displacement difference was estimated to be 0.98 %. The resulting differences are negligible, hence indicating that the accuracy of outputs was comparable.

3. Concerning the TI, it was observed that SMD is more effective in terms of reducing the elapsed time as compared to RK4M. This was demonstrated by TI from RK4M which was approximately 58s longer than that from SMD.

4. SMD was observed to slightly reduce the input earthquake acceleration compared to the acceleration data obtained from SS. This leads to suggesting that “From workspace” block should be revised for better performance.

5. Long-period and long-duration earthquakes need careful and deep investigation, as they showed unusual floor displacements and elastomer shear strains, though their PGAs were small. Therefore, PGA should not necessarily be a good indicator of large floor displacements, unless combined with the earthquake nature. Future studies should deeply investigate the influence of earthquake nature, not only on the responses of the isolated structure but also on the isolator itself such as its material properties.

References

1. Kasimzade, A.A, Tuhta, S. Estimation of Sensitivity and Reliability Base Isolated Building under Earthquake Action. International Symposium on Network and Center-Based Research for Smart Structures Technologies and Earthquake Engineering. Osaka, Japan, 2004. Pp. 407–413.
2. Kasimzade, A.A. Structural Dynamics: Theory and Application to Earthquake Engineering (with CD included for education and dynamic analysis programs). Third Ed. Nobel Publication, 2018. 361 p.
3. Mathews, J.H., Fink, K.D. Numerical Methods Using MATLAB. 4th ed.53(9). Pearson. New Jersey, 2004. 691 p.
4. Gavin, H.P. Numerical Integration in Structural Dynamics. Finite Element Procedures in Engineering Analysis. 2016. Pp. 439–506.
5. Shrimali, M.K., Jangid, R.S. Non-linear seismic response of base-isolated liquid storage tanks to bi directional excitation. Nuclear Engineering and Design. 2002. 217(1–7). Pp. 1–20.DOI: 10.1016/S0029-5493(02)00134-6.
6. Matsagar, V.A., Jangid, R.S. Seismic response of base-isolated structures during impact with adjacent structures. Engineering Structures. 2003. 25(10). Pp.1311–1323. DOI: 10.1016/S0141-0296(03)00081-6.
7. Kasimzade, A.A., Tuhta, S., Atmaca, G. New Structural Seismic Isolation System. Seismic Isolation, Structural Health Monitoring, and Performance Based Seismic Design in Earthquake Engineering: Recent Developments. Springer, 2018. DOI: 10.1007/978-3-319-93157-9
8. Kasimzade, A.A., Dushimimana, A., Tuhta, S., Atmaca, G., Günday, F., Pfidze, K., Abrar, O. A Comparative Study on Effectiveness of Using Horasan Mortar as a Pure Friction Sliding Interface Material. European Journal of Engineering Research and Science. 2019. 4(2). Pp. 64–69. DOI: 10.24018/ejers.2019.4.2.1166.
9. Young, T., Mohlenkamp, M. Introduction to Numerical Math and Matlab Programming. Ohio University, 2009. 193 p.
10. Bangash, M.Y.H. Earthquake Resistant Buildings. Springer. London, 2011. 739 p. DOI: 10.1007/978-3-540-93818-7
11. Smekal, Z. Difference Equations with Forward and Backward Differences and Their Usage in Digital Signal Processor Algorithms. Radioengineering,. 2015. 15(2). Pp. 45–52.
12. Dushimimana, A., Nzamurambaho, F., Shyaka, E., Niyonsenga, A.A. Optimum Performance of Isolation System for Medium Rise Buildings Subject to Long Period Ground Motions. International Journal of Applied Engineering Research. 2018. 13(23). Pp. 16342–16350.
13. Djedoui, N., Ounis, A., Pinelli, J.P., Abdeddaim, M., Mahdi, A., Jean Paul, P. Hybrid Control Systems for Rigid Buildings Structures under Strong Earthquakes. Asian Journal of Civil Engineering. 2017. 18(6). Pp. 893–909.
14. Zhong-ming, X., Xuan, C., Zi-liang, Y. The study of sliding displacement spectrum on sliding base isolation structure. 6th International Conference on Advances in Experimental Structural Engineering, 2015. Pp. 9.
15. Chaturvedi, D.K. Modeling and Simulation of Systems Using MATLAB and Simulink. Taylor & Francis Group 6000. New York, 2010. 734 p.
16. Sina, S. Principal Component and Independent Component Regression for Predicting the Responses of Nonlinear Base Isolated Structures. University of Waterloo, 2008.
17. Nanda, R.P., Agarwal, P., Shrikhande, M. Earthquake Hazard Mitigation for Rural Dwellings by P-F Base Isolation. 14th World Conference on Earthquake Engineering (14WCEE). 11(2)Beijing, China, 2008. Pp. 2–9.
18. Dushimimana, A. The experımental and numerical studies on the effectiveness of aseismic base isolation. Ondokuz Mayis University. 2019 [Online]. URL: http//tez.yok.gov.tr/UlusalTezMerkezi/giris.jsp

19. Mohammadzadeh, A., Valley, G. Solving Nonlinear Governing Equations of Motion Using Matlab and Simulink in First Dynamics Course. American Society for Engineering Education. 2006. 11(2). Pp. 15.
20. Lukashevich, A.A. Modelling of contact interaction of structures with the base under dynamic loading. Magazine of Civil Engineering. 2019. 89(5). Pp. 167–178. DOI: 10.18720/MCE.89.14.
21. Vatin, N.I., Ivanov, A.Y., Rutman, Y.L., Chernogorskiy, S.A., Shvetsov, K. V. Earthquake engineering optimization of structures by economic criterion. Magazine of Civil Engineering. 2017. 76(8). Pp. 67–83. DOI: 10.18720/MCE.76.7.
22. Bayramukov, S.H., Dolaeva, Z.N. Dynamic programming in optimization of comprehensive housing stock modernization. Magazine of Civil Engineering. 2017. 76(8). Pp. 3–19. DOI: 10.18720/MCE.76.1.
23. Jian, F., Xiaohong, L., Yanping, Z. Optimum design of lead-rubber bearing system with uncertainty parameters. Structural Engineering and Mechanics. 2015. 56(6). Pp. 959–982. DOI: 10.12989/sem.2015.56.6.959.
24. Shoaei, P., Tahmasebi, H., Mehdi, S. Seismic reliability-based design of inelastic base-isolated structures with lead-rubber bearing systems. Soil Dynamics and Earthquake Engineering. 2018. 115(June).Pp.589–605. DOI: 10.1016/j.soildyn.2018.09.033.
25. Han, J., Kyu, M., Choi, I. Experimental study on seismic behavior of lead-rubber bearing considering bi-directional horizontal input motions. Engineering Structures. 2019. 198(August). Pp. 109529. DOI: 10.1016/j.engstruct.2019.109529.
26. Yamamoto, Y., Yoshimura, C. Long-Period Ground Motion Simulation of Tokai-Tonankai-Nankai Coupled Earthquake Based on Large-Scale 3D FEM. 15th World Conference on Earthquake Engineering (15WCEE)Lisboa, 2012. Pp. 10.
27. Cheng, X., Jing, W., Li, D. Dynamic response of concrete tanks under far-field, long-period earthquakes. Proceedings of the Institution of Civil Engineers - Structures and Buildings. 2019. Pp. 1–14. DOI: 10.1680/jstbu.18.00024.
28. Hu, R.P., Xu, Y.L. SHM-Based Seismic Performance Assessment of High-Rise Buildings under Long-Period Ground Motion. Journal of Structural Engineering. 2019. 145(6). Pp. 04019038. DOI: 10.1061/(asce)st.1943-541x.0002323.
29. Bai, Y., Guan, S., Lin, X., Mou, B. Seismic collapse analysis of high-rise reinforced concrete frames under long-period ground motions. Structural Design of Tall and Special Buildings. 2019. 28(1). DOI: 10.1002/tal.1566.
30. Rao, P.B., Jangid, R.S. Experimental Study of Base-Isolated Structures. Journal of Earthquake Technology. 2001. 38(1). Pp. 1–15.
31. Tolani, S., Sharma, A. Effectiveness of Base Isolation Technique and Influence of Isolator Characteristics on Response of a Base Isolated Building [Online]. American Journal of Engineering Research (AJER). 2016. (5). Pp. 198–209. URL: www.ajer.org (date of application: 25.10.2019).
32. Friedland, B. Control System Design: An Introduction to State Space Methods. Dover Publications. New York, 1986. 506 p.
33. Butcher, J.C. Numerical Methods for Ordinary Differential Equations. 2nd ed. John Wiley and Sons Ltd, 2003. 484 p.
34. Kang, M.C., Sang-Won, C., Hyung-Jo, J., In-Won, L. Semi-active fuzzy control for seismic response reduction using magnetorheological dampers. Earthquake Engineering and Structural dynamics. 2002. 33. Pp. 723–736. DOI: 10.1002/eqe.372.
35. Nassim, D., Abdelhafid, O., Mahdi, A., Djedoui, N., Ounis, A., Abdeddaim, M. Active Vibration Control for Base-Isolated Structures Using a PID Controller Against Earthquakes. International Journal of Engineering Research in Africa. 2016. 26. Pp. 99–110. DOI: 10.4028/www.scientific.net/JERA.26.99.
36. Dushimimana, A., Gunday, F.. Operational Modal Analysis of Aluminum Model Structures using Earthquake Simulator. International Conference on Innovative Engineering Application (CIEA2018), 2018. Pp. 10.
37. Peter, S., Darina, H. State-Space Model of a Mechanical System in MATLAB/Simulink. Engineering Structures. 2012. 48. Pp. 629–635. DOI: 10.1016/j.proeng.2012.09.563.
38. Kasimzade, A.A., Tuhta, S., Gencay, A. Spherical foundation structural seismic isolation system: development of the new type earthquake resistant structures. 6th international conference on theoretical and applied mechanics (TAM15)Salerno,Italy, 2015.
39. Kasimzade, A.A., Tuhta, S. Stochastic Parametric System Identification Approach for Validation of Finite Element Models : Industrial. 2012. (June 2011). Pp. 41–61.
40. Kalfas, K.N., Mitoulis, S.A., Katakalos, K. Numerical study on the response of steel-laminated elastomeric bearings subjected to variable axial loads and development of local tensile stresses. Engineering Structures. 2017. 134. Pp. 346–357. DOI: 10.1016/j.engstruct.2016.12.015.
41. University of California. Pacific Earthquake Engineering Research Center (PEER) NGA: Ground Motion Database. 2013 [Online]. URL: https://peer.berkeley.edu/peer-strong-ground-motion-databases (date of application: 20.06.2018).
42. Colombo, A., Negro, P. A damage index of generalised applicability. Engineering Structures. 2012. 27. Pp. 1164–1174. DOI: 10.1016/j.engstruct.2005.02.014.
43. EN 1337-3: 2005. Structural bearings – Part 3: elastomeric bearings. Brussels: European Committee for Standardization. 2005.
44. Kumar, M., Whittaker, A.S., Constantinou, M.C. An advanced numerical model of elastomeric seismic isolation bearings. Earthquake Engineering & Structural Dynamics. 2014 [Online]. DOI: 10.1002/eqe.2431. URL: wileyonlinelibrary.com
45. Choun, Y., Park, J., Choi, I. Effects of Mechanical Property Variability in Lead Rubber Bearings on The Response Of Seismic. Nuclear Engineering and Technology. 2014. 46(5). Pp. 605–618. DOI: 10.5516/NET.09.2014.718.
46. BS EN 15129: 2009. Anti-seismic devices. BSI British Standards. 2010.
47. American Association of State Highway and Transportation Officials, AASHTO. Guide Specifications for Seismic Isolation Design. 4th ed.Washington, DC, 2014.
48. Japan Road Association, JRA. Bearing support design for highway bridges. Tokyo, Japan, 2011.

Contacts:

Aloys Dushimimana, +905366560436; chenkodu432@gmail.com
Aude Amandine Niyonsenga, +8617858530159; anaudy92@gmail.com
Gildas Jesuskpedji Decadjevi, +905458418576; gildasdeca@gmail.com
Lilies Kathami Kathumbi, +254780699845; lilieskath@gmail.com